

## Supplementary Information

### Wide tunable lasing in photoresponsive chiral liquid crystal emulsion

Zhi-gang Zheng <sup>a, b, \*</sup>, Bo-wei Liu <sup>a</sup>, Lu Zhou <sup>a</sup>, Wei Wang <sup>a</sup>, Wei Hu <sup>b</sup>, Dong Shen <sup>a, \*</sup>

<sup>a</sup> Department of Physics, East China University of Science and Technology, No.130, Meilong Road, Shanghai, 200237, China.

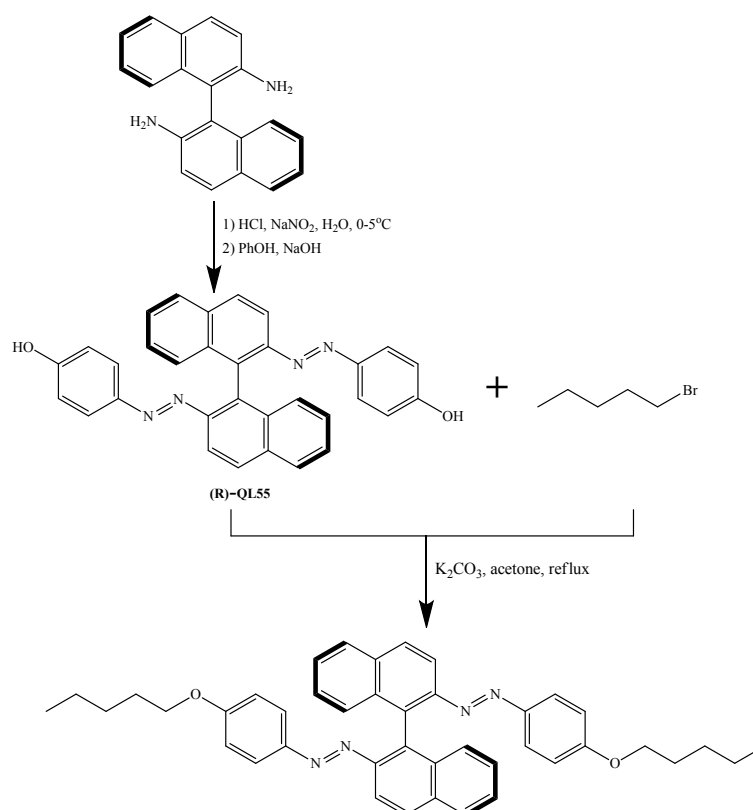
<sup>b</sup> National Laboratory of Solid State Microstructures and College of Engineering and Applied Sciences, Nanjing University, Nanjing 210093, China

\* [zgzheng@ecust.edu.cn](mailto:zgzheng@ecust.edu.cn); [shen@ecust.edu.cn](mailto:shen@ecust.edu.cn)

#### Materials

##### Photoresponsive Chiral Switch QL55

The synthetic route of the photoresponsive chiral switch molecules QL55 is given in Scheme 1:



**Scheme S1.** Synthetic route of QL55.

The chemical structure, identified by <sup>1</sup>H NMR and high resolution mass spectrometer, is shown as follows:

<sup>1</sup>H NMR (CDCl<sub>3</sub>, 400 MHz)  $\delta$ (ppm): 0.89 (t,  $J=7.04$  Hz, 6H, -CH<sub>3</sub>), 1.28~1.42 (m, 8H, -CH<sub>2</sub>-), 1.68~1.76 (m, 4H, -CH<sub>2</sub>-), 3.89 (t,  $J=6.58$  Hz, 4H, -CH<sub>2</sub>-), 6.71 (d,  $J=8.88$  Hz, 4H, Ar-H), 7.23~7.31 (m, 6H, Ar-H), 7.42~7.50 (m, 4H, Ar-H), 7.96 (d,  $J=8.52$  Hz, 2H, Ar-H), 8.04 (d,  $J=8.92$  Hz, 2H, Ar-H), 8.15 (d,  $J=8.92$  Hz, 2H, Ar-H). HRMS

(ESI):  $m/z$  635.3391 [M+H]<sup>+</sup>.

### Photoresponsive Chiral Liquid Crystals (CLCs)

Doping the single dye with wide fluorescence spectrum and good compatibility into CLCs host is a better choice for the wide tunable CLC emulsion based laser. Therefore, 4-(dicyanomethylene)-2-methyl-6-(4-dimethylaminostryl)-4H-pyan (DCM, supplied from Sigma-Aldrich) became a suitable candidate, not only because of the rod-like molecular geometry that enforcing the compatibility, but also the wider emission band spanning from 550 to 680 nm. This means that to achieve the wide tunable lasing, the photo-tuning range of photonic band gap (PBG) should cover the emission band to the largest extent. Generally, increasing the content of photoresponsive chiral switch can widen the tuning range of PBG, however it also reduces the photo-stability of the mixture on the contrary, therefore the content of QL55 should be determined in accordance with the tradeoff between the tunability and the stability. Therefore, in our experiments, the photo-insensitive chiral agent R811 and photosensitive chiral switch QL55 were mixed together, and their optimized contents for were 19.5 wt% and 2.5 wt%, respectively, to simultaneously ensured the wide tuning range and weak photosensitivity; while the content of DCM was controlled at a lower amount of 0.5 wt% for avoiding the fluorescence quenching. The helical twisted power (HTP) for the system was tested through the common method of Grandjean-Cano wedge (supplied by Instec Co., Ltd.). Provided that the HTP for the mixed system, the chiral R811 and the chiral switch QL55 are  $(HTP)_0$ ,  $(HTP)_{811}$ , and  $(HTP)_{QL}$ , respectively; the weight ratio of R811 and QL55 are denoted by  $C_{811}$  and  $C_{QL}$ , respectively; thus the following relationship is satisfied,

$$(HTP)_0 = C_{811}(HTP)_{811} + C_{QL}(HTP)_{QL} \quad (S1)$$

$C_{811}$ ,  $C_{QL}$  and  $(HTP)_{811}$  have been known, while  $(HTP)_0$  can be tested, in consequence,  $(HTP)_{QL}$  can be calculated through Eq. (S1).

### CLC emulsion

For the purpose of obtaining the emulsion with uniform CLC droplets dispersion, 10 wt% of the aforementioned mixture were blended with the aqueous solution of polyvinyl alcohol (PVA, supplied from Sigma-Aldrich) containing 15 wt% PVA, and then emulsified by stirring with the rate of 90 rpm for 5 minutes at room temperature. Subsequently, as schemed in Fig. S1(a), the emulsion was coated onto a clean glass with doctor blade, forming the wet film (Fig. S1(b)) with the thickness of 125  $\mu$ m maintained by Kapton tapes (supported by Dupont), and then deswelling at room temperature for about 1 hour, consequently, obtaining the dry film (Fig. S1(c)) with the thickness of 50~60  $\mu$ m. The film was excited by the pumping beam, and the emission laser was tuned by the LED sources (Fig. S1(d)).

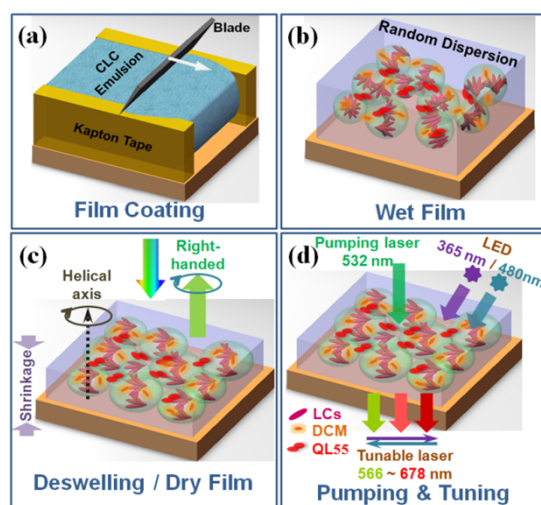


Fig. S1 Schemes of the fabrication and inner structure of the CLC emulsion laser film.

## Optical Setup for Pumping and Photo-tuning

As shown in Fig. S2, the sample was excited by a second-harmonic Q-switched Nd: YAG pulsed laser (supplied by Beamtech Co., Ltd., Canada) with the output wavelength of 532 nm, the pulse width of 6 ns and the repetition rate of 1 Hz. The stray light from the pumping laser was filtered by a pinhole, and the laser was collimated by a spherical lens (L2). A polarizer (P) and a quarter waveplate ( $\lambda/4$ ) was assembled to convert the pump laser to the circular polarization with the opposite rotation sense to the helix of CLCs to avoid reflection caused by PBG. The angle between the transmission axis of polarizer and the fast axis of the waveplate was set to  $45^\circ$ . Subsequently, the pumping laser was splitted into two beams with equal energy by a beam splitter. Both of the beams were focused by the spherical lenses (L3 and L4), the one impinging on the sample (S) as the excitation light and the other, with the same energy, was detected by the energy meter (D1) to test the excitation energy of the sample in real-time. The photo-tuning of the emission was conducted through the irradiation with LED source. Similarly, the LED light was collimated and splitted into two by a beam splitter, one was the exposure light to shift the wavelength of the emission laser, and the other was received by the energy meter to detect the intensity of the photo-tuning. The wavelength and the image of the emission laser was monitored respectively by an optical fiber connected spectrometer and a CCD camera. In this experiment, a variable neutral density filter (NDF) was inserted into the optical path to change the energy of incident pumping laser, and a 532-nm color filter (CF) was set behind the sample to remove the influence of the pumping laser on the testing of the emission.

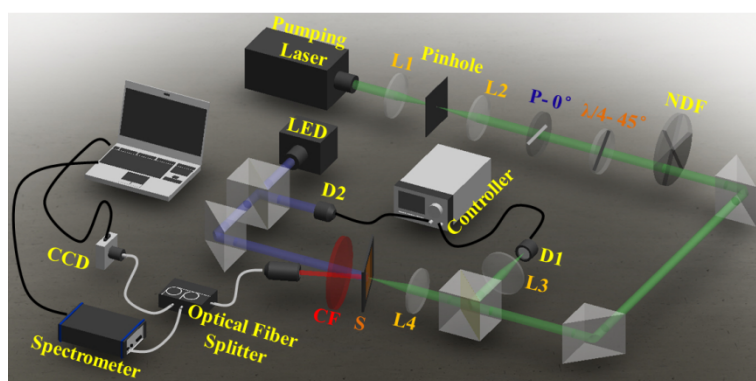


Fig. S2 Pumping and tuning optical setup.

## Molecular dynamic simulations and calculations

Molecular dynamic (MD) methods were adopted to explore the microscopic characteristics of the CLC systems in further. Generally, MD simulations are implemented as the following three steps: firstly, some amounts of molecules are settled into a cubic box with a certain dimensions determined by the density of material. Such cubic box always brings many rebounds because the molecules collide with the walls of the box, thereby changing the moving direction of the molecules during MD process, however, the effect of the walls is inexistent in the real system. Therefore, in order to make the simulations close to the reality, the periodic boundary condition is necessary to be set before the simulations to avoid the influences of the walls in the simulations.<sup>1, 2</sup> Secondly, an appropriate force field need to be selected to move every atom contained in the molecules reaching the most stable position. The force field, a potential energy function of the system, is normally expressed by the coordinates of the center-of-mass, whereby the acceleration, velocity and the displacement of the atoms can be deduced based on Newton's law.<sup>3, 4</sup> At the initiation of MD process, an initial velocity is generated and assigned to the atoms, while keeping the total momentum of the system to be zero; after then these atoms will be restrained by the force field and moved to the next certain position; repeating in this way until the entire system reaches thermal equilibrium. Thirdly, a proper statistical ensemble algorithm is adopted to conduct the thermodynamic relaxation at a defined temperature. After the system reaches equilibrium, there is usually followed by a data collection process, to save

the coordinate of atoms for the convenience of corresponding calculation and analysis.

Based on the aforementioned methods, MD simulations were performed to explore the influences of photoisomerization on the configuration, energy, compatibility (or solubility), and arrangement of the LCs system doped with QL55 chiral switch. For the reason that the photoreaction was caused by the photosensitive QL55, rather than the photo-insensitive chiral agent R811, the ternary mixture of LCs, R811, and QL55 was simplified as the binary mixture of LCs and QL55 in the simulations for cutting the unnecessary calculation and saving the simulation time. The XH-07X used in the experiments is a kind of composite LCs, which makes the simulations complicated, however it has been reported that the main component of such LCs is the common 5CB (>60 mol%) and the birefringence of the LCs ( $\sim 0.169$  @  $25^\circ\text{C}$ ) at room temperature is very close to that of 5CB,<sup>5, 6</sup> thus the composite LCs, XH-07X, was replaced by the single component LCs, 5CB, in consideration both of the accuracy and simplicity for the simulations. Not merely because of this, there are many experimental results can be directly used during calculation as well, thereby facilitating the simulations. It is very difficult to simulate the photoisomerization dynamic process through MD, since such process is so long compared with the intramolecular dynamic process, bringing the huge unnecessary calculation and leading to the waste of simulation time. Actually, the effects of photoisomerization can be investigated by comparing the calculation results of two LCs systems containing the same amount of *trans*-Azo isomers and *cis*-Azo isomers. The simulations for such two systems are rather time-saving, however without any losing of the accuracy. Based on the above considerations, a large cubic box was established, containing 960 5CB molecules and 128 *trans(cis)*-QL55 molecules, with the dimensions of  $80.52 \times 80.52 \times 80.52 \text{ \AA}^3$  determined by the density of the material. This density was approximated as the density of pure 5CB at  $25^\circ\text{C}$  ( $\sim 1.020 \text{ g/cm}^3$ ) herein, since that the minority of QL55, with the proportion only about 10 mol%, which brings so little influence on the density of the mixed system that could almost be ignored in the simulation. The 5CB molecules were originally set as the nematic alignment in the box, and the director was defined as the long axis of molecule. The polymer consistent force field (PCFF), which is very suitable and widely adopted for the simulation of organic molecules containing C, H, O, N, S and halogen atoms, such as the LC molecules, was selected for carrying out the MD simulations.<sup>7-9</sup> The mathematic expression of PCFF can be found in many previous publications. In view of the phase transition of the mixed system, from the nematic to chiral nematic phase due to the chirality of QL55, occurring during the thermodynamic process, NPT ensemble was considered as the more appropriate algorithm since the strong capability to conduct the MD simulation relative to the phase separation.<sup>1-4</sup> The pressure was set as the normal atmospheric pressure, 0.1 MPa; while the relaxation temperature was  $25^\circ\text{C}$  which is consistent with that in experiments. To comply with the minimum image convention, the cutoff radius should be less than a half of the length of cubic box,<sup>3, 4, 10, 11</sup> thus setting such radius as  $40 \text{ \AA}$  is reasonable. With regard to the system containing *cis*-QL55 isomers, an additional constraint should be performed before starting MD simulation, to fix the conformation of *cis*-Azo group contained in *cis*-QL55, for the purpose to avoid the *cis*-to-*trans* thermo-recovery at  $25^\circ\text{C}$ , thus the system after undergoing the *trans*-to-*cis* isomerization can be simulated. That means, without conformation fixing, the *cis*-Azo will transform to the *trans*-isomer during the thermo-relaxation, which deviates the foregoing simulation aim. The entire system was relaxed under the above set conditions to reach the thermo-equilibrium, and subsequently followed by the trajectory collection to obtain the corresponding coordinates for data analysis.

The thermo-equilibrium of the system with the lowest energy at the set temperature can be achieved after the completion of MD simulations. By means of the obtained coordinates from the simulations, the bond length and angle, the out-of-plane dihedral angle, as well as the correlations between them can be calculated through the mathematic expression of PCFF, and thereby the bond energy of the system is obtained, that is the intramolecular action; similarly, the non-bond energy, such as static electronic interaction and the Van der Waals interaction, which are directly determined by the distance between two molecules, also can be calculated through the

coordinates; and the sum of the items of bond and non-bond energies is the total energy of the system. Provided that the total energy of the system is denoted as  $E_0$ ; the energy of LCs and QL55 are  $E_{LC}$  and  $E^*$ , respectively; therefore, the interaction between LCs and QL55,  $E_{int}$ , is deduced as Eq. (S2),<sup>12</sup>

$$E_{int} = E_0 - (E_{LC} + E^*) \quad (S2)$$

The miscibility between two materials can be estimated as well by calculating and comparing their cohesive energy density (denoted as  $E_c$  herein), which is defined as the energy needed to completely remove the molecular interactions within the unit volume of condense matter.<sup>13</sup> In other words, cohesive energy density is similar to the gasification energy for the condense matter in the unit volume. The mathematic expression of PCFF is used in the calculation of  $E_c$ . If defining the solubility parameter ( $\delta$ ) as the square root of cohesive energy density, as shown in Eq. (S3), thus the materials with the similar solubility parameters have the better miscibility, and vice versa.

$$\delta = E_c^{1/2} \quad (S3)$$

LC molecular director is defined as the direction parallel to the long axis. Therefore, based on the definition, the director for every molecule can be calculated from the coordinates of the two atoms on the long axis. And consequently, the order parameter ( $S$ ) for the defined LCs system can be easily obtained in accordance with the conventional Legendre polynomials expanded to second order, as shown in Eq. (S4),<sup>14</sup>

$$S = \frac{1}{2} (3 \langle \cos^2 \theta_{ij} \rangle - 1) \quad (S4)$$

where,  $\theta_{ij}$  is the angle between the directors of any two LC molecules, which is calculated through the molecular directors; while the angle brackets,  $\langle \dots \rangle$ , means the statistical average.

### Absorption spectrum of CLCs doped with QL55

The absorption spectrum of CLCs doped with 2.5 wt% QL55 was tested for determining the photosensitive wave band of the mixture. Similar with the majority of Azo-doped LCs, two evident absorption bands appear in the ultraviolet-visible (UV-Vis) band, locating at near UV and blue-green wave band. The blue curve in Fig. S3 shows a high-absorption band, range from 310 nm to 420 nm, with the peak at 360 nm, as well as a low-absorption band, range from 420 nm to 540 nm, with a mild peak at ~470 nm. As the mixture was irradiated by 365-nm-LED, the peak at near UV band (310~420 nm) decreased, while accompanied by the rising of the peak at visible band (420~540 nm), corresponding to the photoisomerization from *trans* to *cis*. In contrast, irradiating with 480-nm-LED led to a recovery of the absorption spectrum, caused by the reverse transforming from *cis* to *trans*. If continually exposing the mixture until the spectrum was invariant, the sample reached PSS. The red and dark-green curves in Fig. S3 show two absorption behaviors of PSS<sub>UV</sub> and PSS<sub>VIS</sub>, respectively. Undoubtedly, significant changes on absorbance were presented between two PSS. However, it was also found that the spectrum of PSS<sub>VIS</sub> cannot overlap well with that of initial state (the blue curve), showing a weaker absorption at the near UV band. We ascribe such difference to the incomplete recovery of *cis*-QL55 under the visible light exposure. For a complete recovery, the longer thermal relaxation time, normally tens of hours, is necessary.

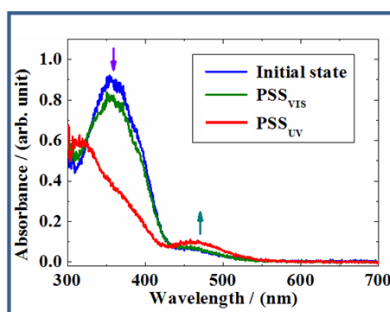


Fig. S3 The absorption spectra of photoresponsive CLCs.

### Transmission spectrums of the deswelling dry film

Figure S4(a) presents the red-shifting of the spectrums when the sample underwent 3 seconds, 14 seconds and 30 seconds irradiation with 365-nm-LED; while Fig. S4(b) gives the blue-shifting of the spectrums corresponding to the recovery of the sample after 5 seconds, 7 seconds and 11 seconds irradiation by 480-nm-LED source. The larger decay of transmittance in the range from 500 nm to 550 nm is caused by the absorption of laser dye, DCM.

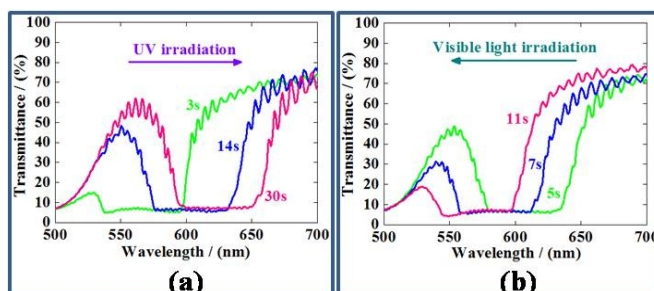


Fig. S4 Spectral shifting of the deswelling film during UV irradiation (a) and visible light irradiation (b).

### References

- 1 M. Hotokkka, 2002, *Molecular Dynamics Simulations*. (Cambridge University Press: Cambridge).
- 2 N. Metropolis, A. W. Rosenbluth, M. N. Rosenbluth, A. H. Teller, *J. Chem. Phys.*, 1953, **21**, 1087.
- 3 J. A. Fay, 1965, *Molecular Thermodynamics*. (Addison-Wesley Publishing Company, Inc.: New York).
- 4 D. C. Young, 2001, *Computational Chemistry*. (John Wiley & Sons: New York).
- 5 S. S. Patnaik, R. Pachter, *Polymer*, 1999, **40**, 6507.
- 6 Z. Zheng, C. Wang, D. Shen, *J. Mater. Chem. C*, 2013, **1**, 6471.
- 7 J. R. Hill, J. Sauer, *J. Phys. Chem.*, 1994, **98**, 1238.
- 8 M. J. Hwang, T. P. Stockfisch, A. T. Hagler, *J. Am. Chem. Soc.*, 1994, **116**, 2515.
- 9 H. Sun, S. J. Mumby, J. R. Maple, A. T. Hagler, *J. Am. Chem. Soc.*, 1994, **116**, 2978.
- 10 C. L. Chen, H. L. Chen, C. L. Lee, J. H. Shin, *Macromolecules*, 1994, **27**, 2087.
- 11 C. L. Chen, H. L. Chen, C. L. Lee, J. H. Shin, *Macromolecules*, 1994, **27**, 7872.
- 12 R. A. Alberty, 1983, *Physical Chemistry*. (John Wiley & Sons: New York).
- 13 J. H. Yin, Z. S. Mo, 2001, *Modern Polymer Physics*. (Sciences Press: Beijing).
- 14 D. Rigby, R. J. Roe, *J. Chem. Phys.*, 1988, **89**, 5280.